Multi-Stage Swirling Fluidized Bed: Part 1 - Numerical Analysis Procedure

Muhamad Silmie Mohamad Shabri[1], Mohd Al Hafiz Mohd Nawi[2,*], Mohd Shahir Kasim[3], Khor Chu Yee[2], Mohd Uzair Mohd Rosli[2], Mohammad Azrul Rizal Alias[1], Raja Muhammad Zulkifli Raja Ibrahim[1]

[1] Faculty of Mechanical Engineering & Technology, Universiti Malaysia Perlis (UniMAP), Kampus Alam UniMAP, Pauh Putra, 02600 Arau, Perlis, Malaysia
[2] Simulation and Modelling Research Group (SiMMREG), Faculty of Mechanical Engineering & Technology, Universiti Malaysia Perlis (UniMAP), Kampus Alam UniMAP, Pauh Putra, 02600 Arau, Perlis, Malaysia
[3] Faculty of Innovative Design and Technology, Universiti Sultan Zainal Abidin, 21300 Terengganu, Malaysia

ARTICLE INFO	ABSTRACT
	Swirling Fluidized Bed (SFB) is a system that possess a plenum chamber and distributor air gap which leading up to dispersion of the airflow to the bed. The current SFB is in contrast with conventional fluidization systems whereby the effect of multi-stage through blades inclination angle (15°) and number of blades (60) was carried out. The simulation was used to compute and assess the performance outcomes of velocity distribution in a SFB. Therefore, the present study focuses on the numerical analysis procedure on the air flow distribution impacted by annular blade distributor arrangement in a Multi-stage SFB via ANSYS Fluent before a detailed study on selected variable would be carried out. As a consequence, the findings of the primary study that have been conducted are in line with expectations formed by earlier research.

1. Introduction

One of current technologies in fluidization systems is Swirling Fluidized Beds (SFB) [1] that were suggested to aid in swirl motion in fluidized beds. The concept of SFB is based on distributors [2] used in conventional fluidization which is proposed to evenly distribute fluidizing the air flow throughout the bed. Through a swirling motion that had an impact on this particular blade arrangement, air distribution in the plenum interacted with each other. Reminds to coventional fluidization systems, most of the design's allowed for easy airflow around the bed, although this led to poor bed usage.

Furthermore, what usually goes to the old fluidization systems when the air velocity is suddenly increased, the airflow seems to be non-uniform. Due to this circumstance, a bubble may form inside the beds [2]. To overcome this circumstance, previous researcher has proposed a new fluidization system that is Swirling Fluidized Beds (SFB) [1-2]. With SFB, the bed distributor is minimized due to the absence of drag. Following the passage of the blade distributor, the optimal performance in terms

---

* *Corresponding author.*
E-mail address: alhafiznawi@unimap.edu.my

of pressure drops and flow actions may be attained by configuring SFB with the needed blade distributor configuration [3]. By referring to the previous experimental study that has been done to the existing SFB system, an advanced on multi-stage SFB had been carried out. Therefore, in current study, the author would investigate the air flow characteristic when using multi-stage SFB based on previous researcher had done [3-6].

Therefore, further numerical simulation studies on the multi-stage blade distributor in the plenum chamber will elucidate more information on the airflow behaviour. On the basis of the current of the Swirling Fluidized Bed, the multi-stage SFB has been developed [6] to enhance the fluidization process and function of SFB. The thorough multi-stage fluidization interaction approach gives a realistic representation of the interaction between airflow and fluidization systems [6-9]. Fig. 1 shows the annular blade distributor with a conical center body
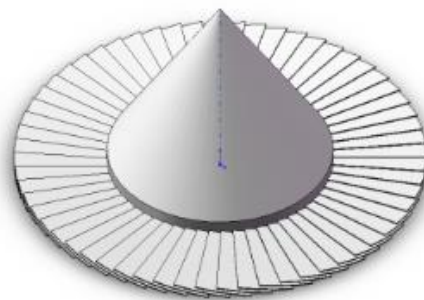
Fig. 1. Annular blade distributor with
a conical center body

2. Methodology
2.1 Numerical Simulation Process

A flow chart of the research processes is presented in Figure 2. The final phase in this research is described as the post-processing phase, employing many different graphical approaches such as grids, contours, vectors, and line plots.

2.2 Description of the Multi-Stage SFB

Using ANSYS Fluent commercial CFD software [10], the airflow distribution in an SFB was evaluated [11] and be used to construct the computation domain and generate the grid. Figure 3 illustrates how the number of blades distributed at 60 is applied in this research. The air intake for velocity boundary condition was simulated using a 2.25 m/s that equal to mass flow rate, 0.22 kg/s and the pressure outlet was set at atmospheric pressure (101,325 Pa). Consequently, the present investigation's flow is consistent and viscous. Thus, the fluid element's density and time do not fluctuate as the air flow moves over the geometrical volume. In addition, the no-slip shear condition assumes that the fluid velocity relative to the geometric boundary is zero. In addition, the wall motion was set to be stationary. In this research, several sorts of angles were employed, including horizontal inclination. In this study, a constant horizontal inclination angle of 15° was used.
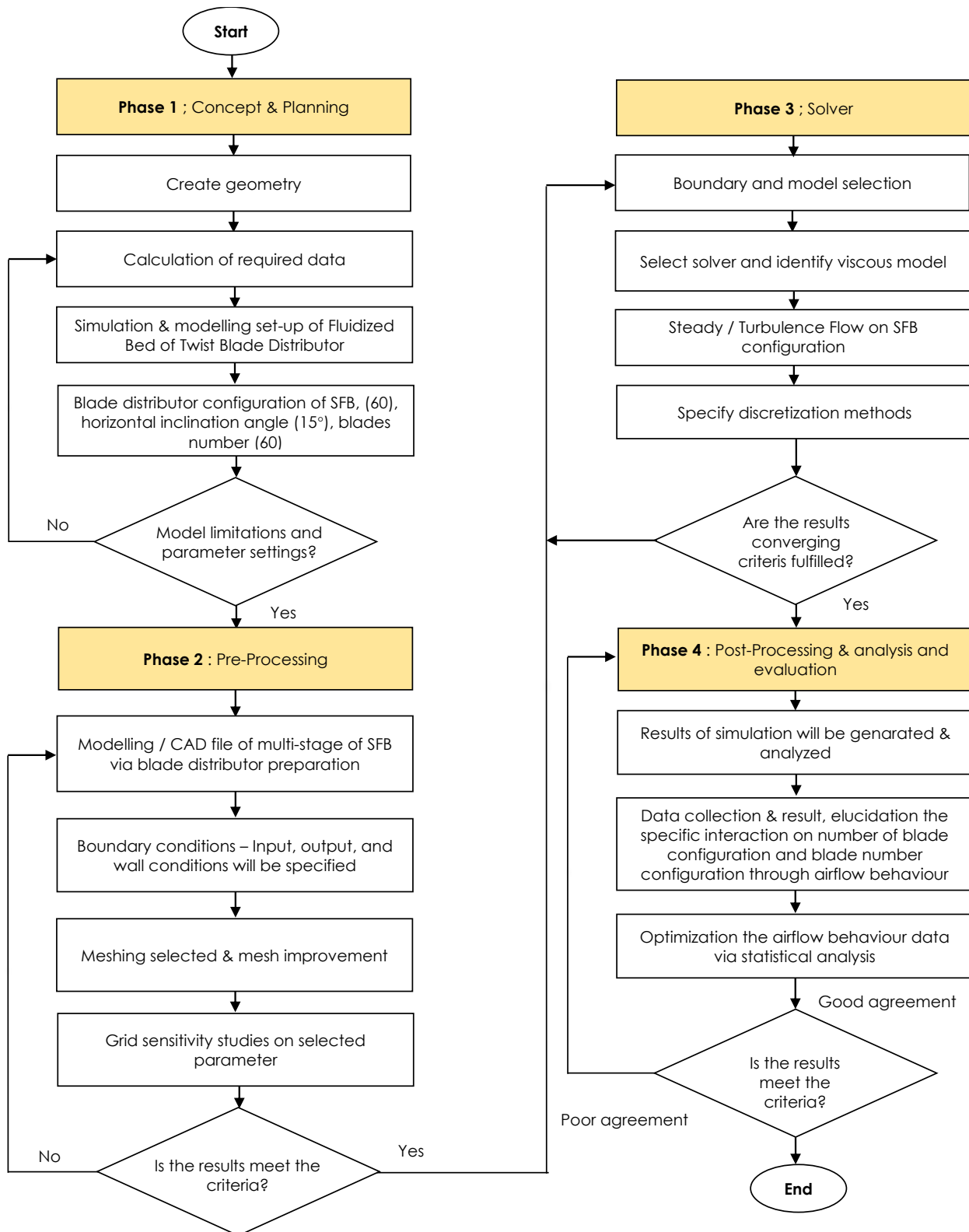
Fig. 2. Flow chart of the research methodology

The horizontal angle was selected based on [1-3]. As a consequence of the preceding study, a full-scale model was constructed. In this research, the kind of blade was modified to an angle blade distributor that matched a turbine blade. One parameter of the blade has been constructed and positioned in the vicinity of the plenum SFB. The SFB's plenum has a diameter of 300 mm [1-3, 5, 6]. Each blade is 2 mm thick and is placed clockwise with a 15° [1] horizontal angle. Based on earlier

studies [2, 3], the angle degree of the blade distributor was decided. Previous studies have shown that a 15° angle via 60 blades number produces high tangential velocity and high velocity magnitude consistency. Therefore, the parameter setting above has been used in current study. The value ratio of the chamber diameter to the radius of the blade distributor (50 mm) was used to collect more data on the influence of the present design study centred on the angle of blade configuration. Boundary conditions of blade distributor column with 60 blades.
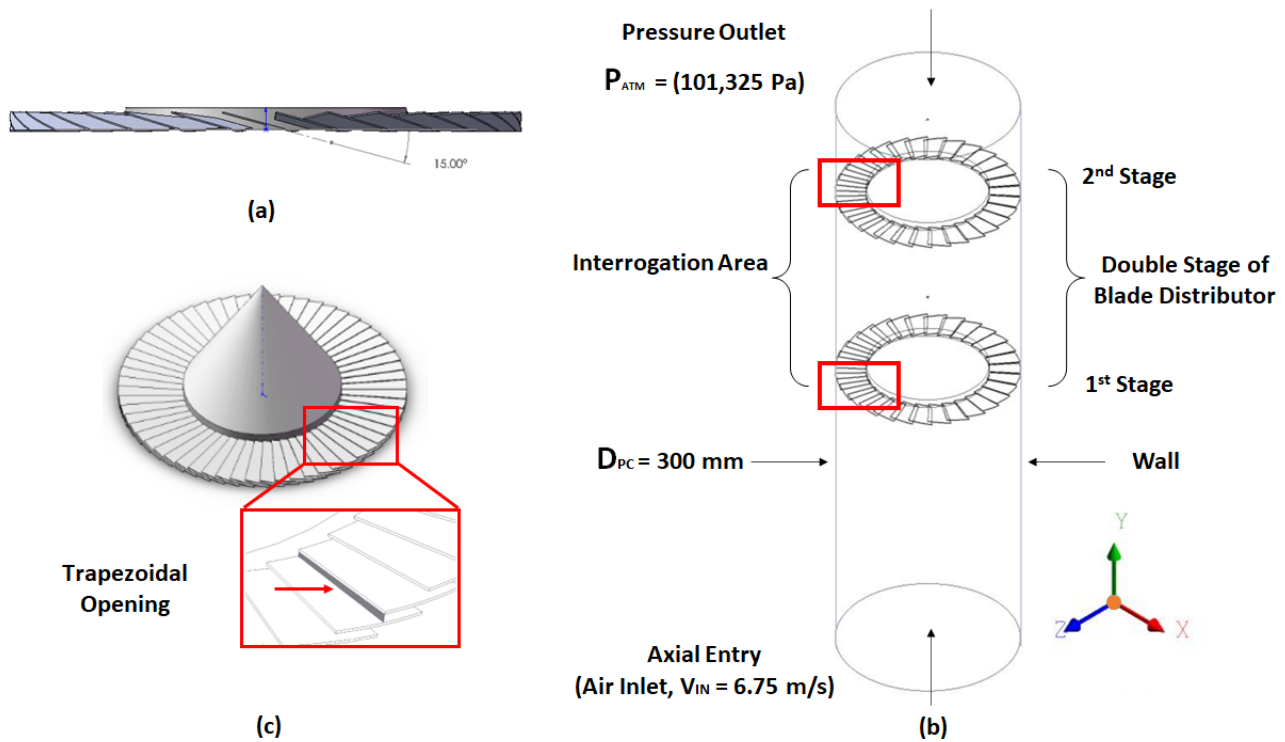
Fig. 3. Fluidization systems (a) Blade inclination angle,15° (b) Boundary conditions of blade distributor 60 blades and (c) Data extraction located at 15 mm above the distributor

2.3 Numerical Model

As a consequence of the present investigation, researchers [3, 5] used a comparable condition setup. The ANSYS Fluent commercial CFD software [10] was able to generate a face mesh consisting of irregular triangular mesh elements by applying the Tri: Pave Meshing Scheme on the surface and the geometry volume. The Tet/Hybrid parameter type defines tetrahedral, hexahedral, pyramidal, and wedge components for the meshing process. Fluidization systems' turbulent flow was simulated using a steady-state segregated implicit solver. In the ANSYS Fluent features, the Reynolds Averaged Navier Stokes (RANS) [12] turbulence equation of the (Re-Normalization Group) RNG techniques based on model transport equations for the turbulence kinetic energy (k) and its dissipation rate (ε) has been selected. To limit numerical diffusion, a second-order upwind technique was selected for the discretization of momentum equations [12].

The methods for pressure-velocity interaction were then resolved using the SIMPLE algorithm. The assessment of meshing is the same as in the previous studies, with the exception of the following facts [5]. The quality of the mesh may be deemed good based on this evaluation. This turbulence model is analogous to that shown in the next subtopic.

2.4 Governing Equation

The current study's governing equations [12] are three-dimensional momentum and continuity equations in cylindrical coordinates that were solved for Newtonian, incompressible fluid in steady flow.

2.4.1 Navier-stoke equation for steady flow case

(r-direction)

$$\rho\left(v_r\frac{\partial v_r}{\partial r}+\frac{v_\theta \partial v_r}{r\partial\theta}-\frac{v_\theta^2}{r}+v_z\frac{\partial v_r}{\partial z}\right)=-\frac{\partial P}{\partial r}+\rho g_r+\mu\left[\frac{1}{r}\frac{\partial}{\partial r}\left(r\frac{\partial v_r}{\partial r}\right)-\frac{v_r}{r^2}+\frac{\partial^2 v_r}{r^2\partial\theta^2}-\frac{2\partial v_\theta}{r^2\partial\theta}+\frac{\partial^2 v_r}{\partial z^2}\right] \quad (1)$$

(ø-direction)

$$\rho\left(v_r\frac{\partial v_\theta}{\partial r}+\frac{v_\theta \partial v_\theta}{r\partial\theta}+\frac{v_r v_\theta}{r}+v_z\frac{\partial v_\theta}{\partial z}\right)=-\frac{1}{r}\frac{\partial P}{\partial\theta}+\rho g_\theta+\mu\left[\frac{1}{r}\frac{\partial}{\partial r}\left(r\frac{\partial v_\theta}{\partial r}\right)-\frac{v_\theta}{r^2}+\frac{\partial^2 v_\theta}{r^2\partial\theta^2}+\frac{2\partial v_r}{r^2\partial\theta}+\frac{\partial^2 v_\theta}{\partial z^2}\right] \quad (2)$$

(z-direction)

$$\rho\left(v_r\frac{\partial v_z}{\partial r}+\frac{v_\theta \partial v_z}{r\partial\theta}+v_z\frac{\partial v_z}{\partial z}\right)=-\frac{\partial P}{\partial z}+\rho g_z+\mu\left[\frac{1}{r}\frac{\partial}{\partial r}\left(r\frac{\partial v_z}{\partial r}\right)+\frac{\partial^2 v_z}{r^2\partial\theta^2}+\frac{\partial^2 v_z}{\partial z^2}\right] \quad (3)$$

2.4.2 Continuity equation

$$\frac{\partial\rho}{\partial t}+\frac{1}{r}\frac{\partial(\rho r u_r)}{\partial r}+\frac{1}{r}\frac{\partial(\rho u_\theta)}{\partial\theta}+\frac{\partial(\rho u_z)}{\partial z}=0 \quad (4)$$

3. Results

The conclusions of the numerical analytic inquiry are reviewed in this section. The tangential velocity of the multi-stage SFB was examined in this study. Data was retrieved on a horizontal plane 15 mm above the distributor since this was the optimal location for analysing the air flow characteristics.

3.1 Grid Independence Study

A grid sensitivity study was carried out in order to determine an effective meshing approach that causes low computational errors owing to truncation and round-off errors while requiring less time to calculate. As shown in Table 1, the most suitable meshing method was selected as the standard scheme to be used and Figure 4(a) for meshing of multi-stage SFB with their respective scheme. The sensitivity analysis, as shown in Table 1, suggests that scheme D is the most suitable scheme for all case studies (which contains cell elements of 1,502,506). The iteration time of 300 iterations in Scheme D is ideal. Moreover, it provides the best size function of all the schemes. Due to these attributes, scheme D has the best and most efficient simulation time, hence minimising the time necessary to simulate each case. This may be observed on the graph as shown in Figure 4(b), where the velocity magnitude results from various systems exhibit the same patent with one another.

Table 1
All different scheme meshing parameter

Meshed Scheme	Number of Elements
Scheme A	422,709
Scheme B	1,461,332
Scheme C	343,893
Scheme D	1,502,506
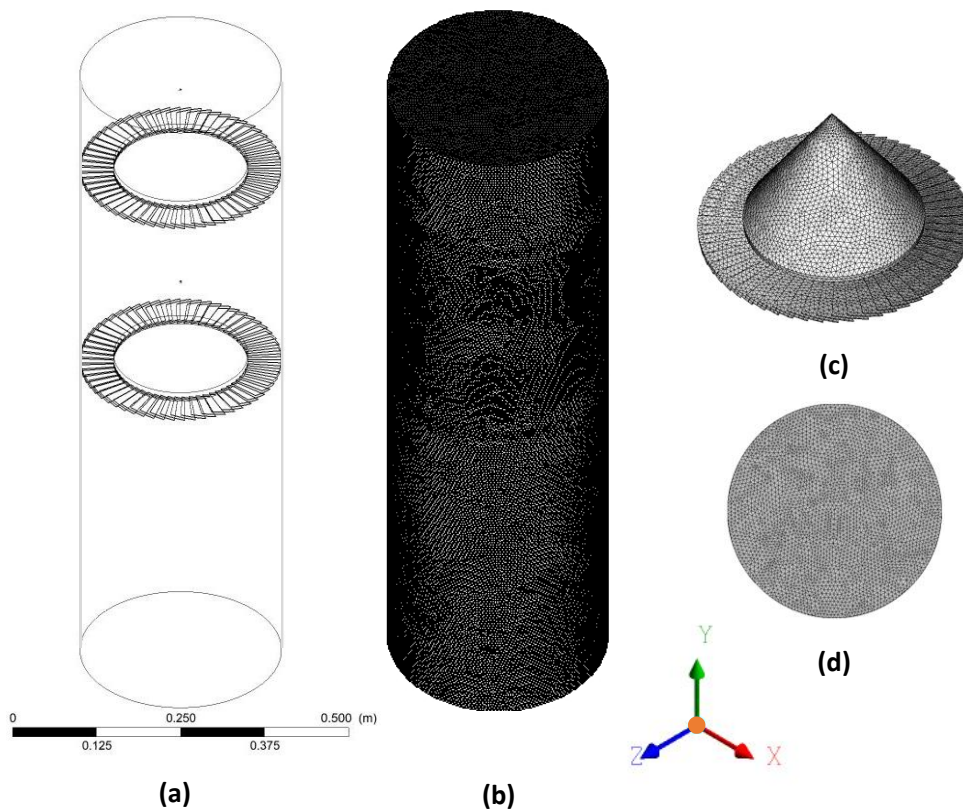
Fig. 4(a). Meshing of multi-stage SFB with their respective scheme (a) SFB domain (b) SFB volume (c) annular blade distributor with a conical center body and (d) inlet meshes
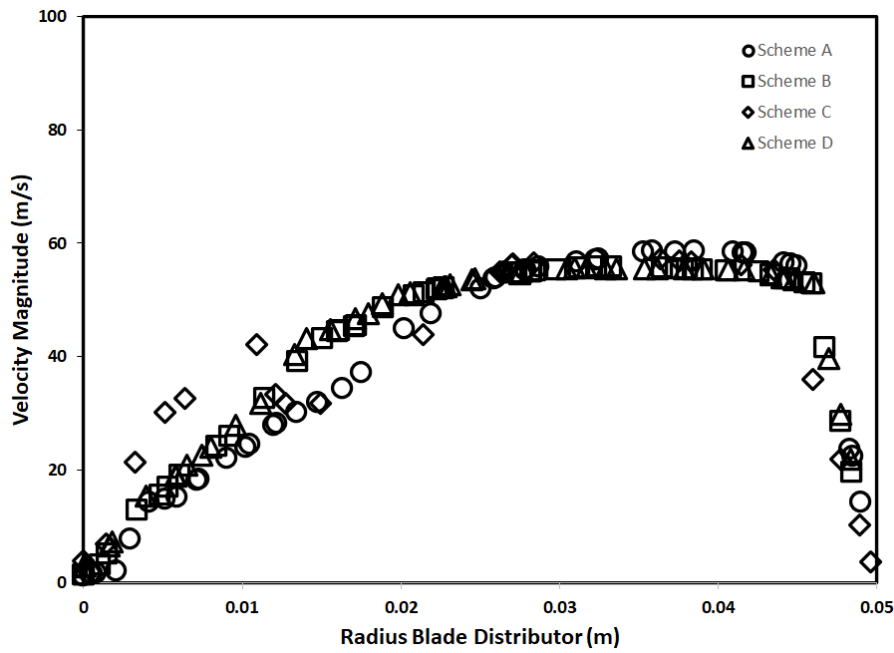
Fig. 4(b). Velocity distribution for a different number of the grid
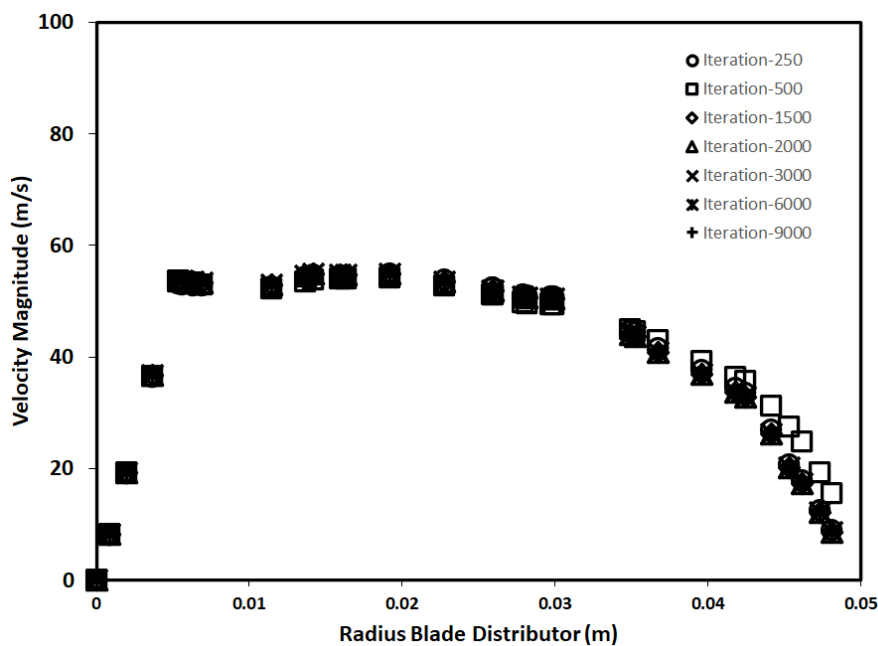
Fig. 4(c). Velocity distribution at various number of iterations

3.2 Turbulence Model Selection

In the selection of turbulent models, all selected models (five total turbulent models, five eddy viscosity models, and one Reynolds Stress Model (RSM) were compared. The eddy viscosity models consist of the standard standard $k–\varepsilon$, realisable $k–\varepsilon$, and RNG $k–\varepsilon$ model. All models show the greatest agreement with the present observation, which is a high-velocity system near the wall, as shown in Figure 5. In actuality, the flow in this region shows forced vortex behaviour due to the vortex's centrifugal influence, which was created by the inclination angle of the blade distributor. In fact, as indicated by previous studies [5], the RNG $k–\varepsilon$ model provides more agreement in the annular blade distributor area.
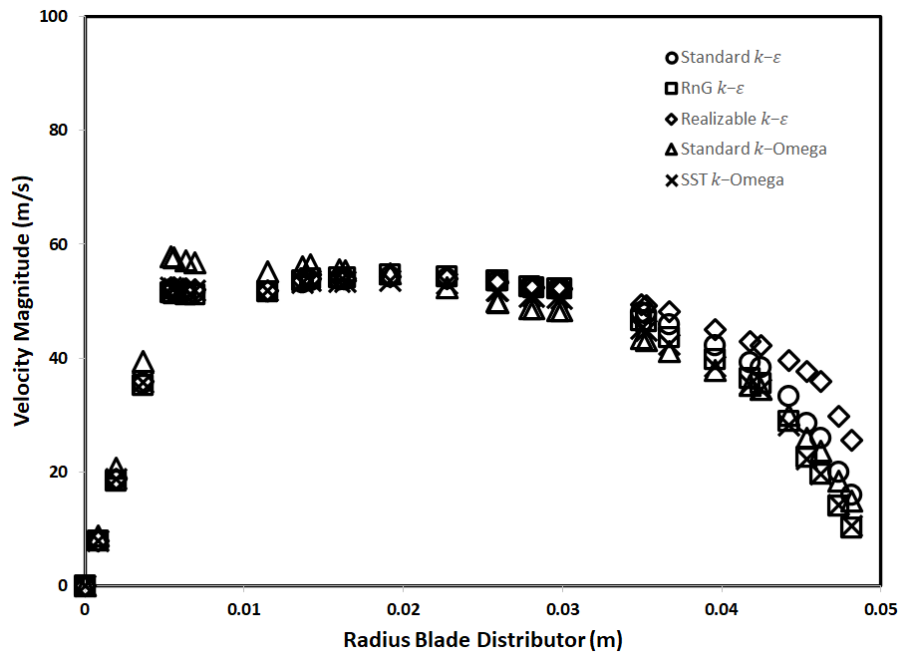
Fig. 5. Velocity distribution at various number of turbulence models

The flow is identifiable in such a region. It is vital to note that the most significant mean flow phenomena occur close to the centreline (e.g., vortex, breakdown, and recirculation zone) (e.g., vortex, breakdown, and recirculation zone). As a result, the RNG $k-\varepsilon$ model is the optimal turbulent model for assessing the flow phenomena at the blade distributor, which is the subject of this paper. The RNG $k-\varepsilon$ model and the conventional $k-\varepsilon$ model share a similar structure. In addition, the inclusion of the component in its equation would significantly improve the accuracy for rapidly strained flows and provide an analytical formula for turbulence Prandtl numbers. It is also appropriate for swirl and turbulence conditions, which are already accounted in the RNG model [5].

The Reynolds Averaged Navier Stokes (RANS) turbulence equation model being considered to be employed in this study is the RNG $k-\varepsilon$ model. The RNG $k-\varepsilon$ model was the most prominent turbulence model applied and taken into consideration in the industry-standard CFD model. It has proven to be dependable, numerically powerful, and has a clear system of predictive capability. The model follows to the settings of the preceding turbulence model study and offers a decent compromise between accuracy and resilience for general-purpose simulations [2, 12].

3.3 Reynolds Number (Re)

Since the distributor blades are oriented to a certain degree, the number of Reynolds (Re) greatly affects the flow characteristics across them. Previous researcher had performed a series of air flow study using a several range of entering plenum chambers with varying blade counts and blade inclination angles (10°, 12°, and 15°). As the flow approaches, there is a vertical component at the entrance of the trapezoidal area between the two blade distributors. No-slip conditions will be considered on this flow direction. Low Reynolds numbers from the flow's impact on the wall led to the formation of a tiny vortex outside the distributor's entrance and a slight constriction of the flow's streamlines in the distributor's direction. As the Reynolds number climbs, the increasing flow momentum will drive the centerline of the vortex to ascend above the horseshoe vortex. The flow would centrifugally go to the wall after the slotted duct distributor.

According to the present study, when there are many blades and a low slotted inclination angle, a huge vortex forms at the top of the blade distribution zone. Keep in mind that the imposed velocity has a significant influence on the flow in this range of Reynolds numbers. The current analysis indicates that a massive vortex arises at the top of the blade distribution region when there are a large number of blades and a low slotted inclination angle. Keep in mind that, in this range of Reynolds numbers, the imposed velocity has a major impact on the flow. The effects of Reynolds number, a simulation's raw data was also performed at several speeds of 2.25 m/s, 5.0 m/s, 6.75.0 m/s, 19.61 m/s and 45.0 m/s respectively that corresponding to 14 881.8, 33 070.6, 44 645.3, 129 702.8 and 297 635.3 Reynolds number, calculated from Eq. (5).

$$Re = \rho V_I D_H / \mu \tag{5}$$

where the dynamic viscosity, μ, density of air, ρ, hydraulic diameter tube ($D_H = 2(r_o - r_i)$) and velocity inlet, V_I were taken in accordance with the velocity inlet above. Therefore, this value showed an effect of fluid turbulence (Re > 4000) for all cases in the current work. As shown in Figure 6, the turbulence model provides a reading result that is quite similar to the RNG $k-\varepsilon$ turbulence model's.
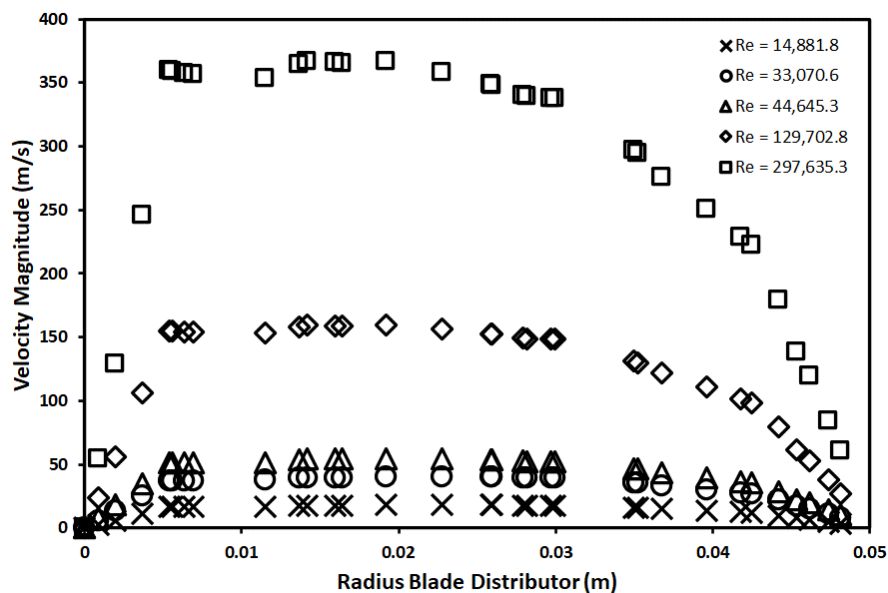
Fig. 6. Velocity distribution at various Reynolds numbers

3.4 Velocity Distribution Analysis

The current study has performed 60 blades with a constant horizontal inclination of 15° in multi-stage SFB. Figure 3 depicts the geometry of the simulation. The air will be diverted as soon as it enters the distributor, producing a whirling effect. This will affect the outer mass of the column created by centrifugal force. Three (3) components comprise the velocity distribution: tangential velocity, radial velocity, and axial velocity. In actual industrial applications, axial velocity promotes fluidization whereas tangential velocity results in a swirling motion. Radial velocity would be attributable to the centrifugal force generated by the whirling gas. In the next study, these velocity components details will be discussed in more depth (Part 2 - Air Flow Distribution).

The distributor blade being dislocated by the air when it is inserted axially may be referred to as the velocity magnitude component. Consequently, the annular blade distributor generates the swirling the air flows. In addition, the swirling movement adds mass to the air at the farthest edge of the column by centrifugal force, causing the flow to separate into its three (3) component components. Figure 7 illustrates the gathered data. As the distributor induces spinning, the air that enters the chamber axially is deflected. Due to the air's centrifugal whirling action near the edge of the base, the flow would break into three (3) velocity components as indicated before. The position of the velocity components retrieved from the data was normalised in line with a previous work by [5]. The statistical analysis may be employed in this research to optimise the present model of current fluidization systems. The optimal design and parameter will be identified, as in earlier studies [13-15].
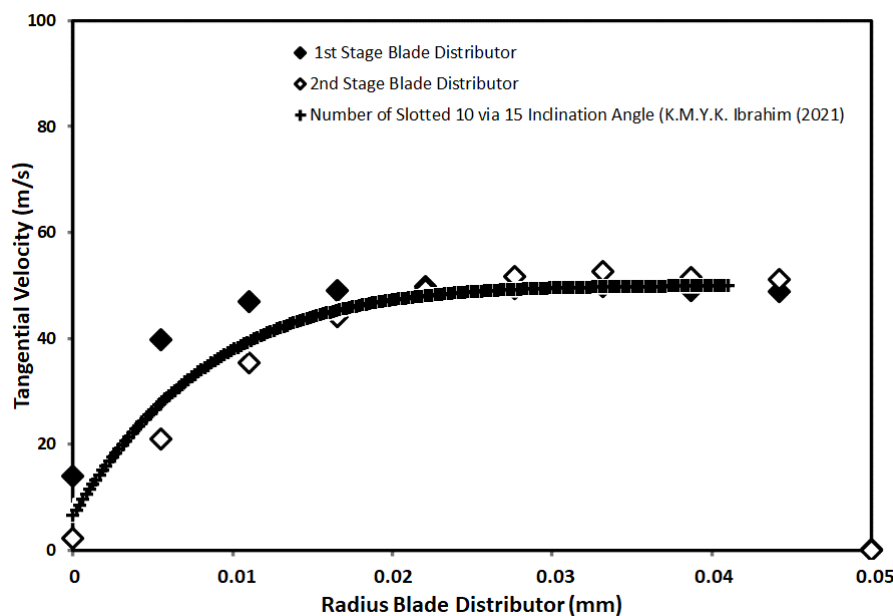
Fig. 7. Velocity magnitude for blade numbers, N_B = 60 with horizontal blade inclination, I_H = 15°

4. Conclusions

The primary objective of this research is to demonstrate the process step and identify the parameter of the present fluidization systems of multi-stage SFB using the commercial CFD programme ANSYS Fluent. A chosen one of the geometries of multi-stage SFB was investigated in order to evaluate one of the key outcomes, namely the retention capability on velocity profile of multi-stage SFB. According to the numerical findings, current fluidization systems have a high retention capacity and velocity homogeneity on the plane of interest. Consequently, a selection of numerical setup settings based on Reynolds number, iterations, scheme, and turbulence model findings has been made, as it is anticipated that this would result in optimal performance characteristics of a multi-sage swirling fluidized bed.

References

[1] Sreenivasan, Binod, and Vijay R. Raghavan. "Hydrodynamics of a swirling fluidised bed." *Chemical Engineering and Processing: Process Intensification* 41, no. 2 (2002): 99-106. https://doi.org/10.1016/S0255-2701(00)00155-0

[2] Mohideen, M. F., and V. R. Raghavan. "Experimental studies on a swirling fluidized bed with annular distributor." *J. Appl. Sci.* 11, no. 11 (2011): 1980-1986. https://doi.org/10.3923/jas.2011.1980.1986

[3] Batcha, Mohd Faizal Mohideen, M. A. M. Nawi, Shaharin Anwar Sulaiman, and Vijay R. Raghavan. "Numerical investigation of airflow in a swirling fluidized bed." *Asian Journal of Scientific Research* 6, no. 2 (2013): 157-166. https://doi.org/10.3923/ajsr.2013.157.166

[4] Abd Latif, Muhammad Lutfi, Mohd Al Hafiz Mohd Nawi, Wan Azani Mustafa, Mohd Sharizan Md Sarip, Mohd Aminudin Jamlos, Masniezam Ahmad, Ku Mohammad Yazid Ku Ibrahim, and Hazizul Hussein. "Numerical analysis of velocity magnitude in a swirling fluidized bed with spiral blade distributor." *Journal of Advanced Research in Fluid Mechanics and Thermal Sciences* 59, no. 1 (2019): 38-44.

[5] Mohd Nawi, Mohd Al-Hafiz. "Aerodynamics of a swirling fluidized bed." PhD diss., Universiti Tun Hussein Malaysia, 2013.

[6] Ashri, S. F. "The Effectiveness of multi-staged swirling fluidized bed. B. Eng." PhD diss., Dissertation. Unversiti Teknologi PETRONAS. Tronoh, Perak, 2012.

[7] Wu, Gongpeng, Wei Chen, and Yan He. "Investigation on gas–solid flow behavior in a multistage fluidized bed by using numerical simulation." *Powder Technology* 364 (2020): 251-263. https://doi.org/10.1016/j.powtec.2020.01.078

[8] Samal, D. K., Y. K. Mohanty, and G. K. Roy. "Study on Multi-stage Liquid-solid semi-fluidization with spherical particles." *Int J Adv Res Dev* 1, no. 10 (2016): 15-20.

[9] Nawi, M. A. M., Muhammad Ikman Ishak, M. U. Rosli, Nur Musfirah Musa, Siti Nor Azreen Ahmad Termizi, C. Y. Khor, and M. A. Faris. "The effect of multi-staged swirling fluidized bed on air flow distribution." In *IOP Conference Series: Materials Science and Engineering*, vol. 864, no. 1, p. 012194. IOP Publishing, 2020. https://doi.org/10.1088/1757-899X/864/1/012194

[10] ANSYS UK Ltd. ANSYS 18: ANSYS Fluent Tutorial Guide Introduction. Canonsburg (U.K): Release 18.0 January 2017.

[11] Kumar, S. Harish, and D. V. R. Murthy. "Minimum superficial fluid velocity in a gas–solid swirled fluidized bed." *Chemical Engineering and Processing: Process Intensification* 49, no. 10 (2010): 1095-1100. https://doi.org/10.1016/j.cep.2010.08.013

[12] Versteeg, Henk Kaarle, and Weeratunge Malalasekera. *An introduction to computational fluid dynamics: the finite volume method*. Pearson education, 2007.

[13] Hazwan, M. H. M., Z. Shayfull, M. A. M. Nawi, M. Ahmad, Mohamad Syafiq AK, and A. M. Roslan. "Warpage optimization on battery cover using genetic algorithm (GA)." In *AIP conference proceedings*, vol. 2129, no. 1, p. 020195. AIP Publishing LLC, 2019. https://doi.org/10.1063/1.5118203

[14] Shayfull, Z., M. H. M. Hazwan, M. A. M. Nawi, M. Ahmad, Mohamad Syafiq AK, and A. M. Roslan. "Warpage optimization on battery cover using glowworm swarm optimisation (GSO)." In *AIP conference proceedings*, vol. 2129, no. 1, p. 020100. AIP Publishing LLC, 2019. https://doi.org/10.1063/1.5118108

[15] Ibrahim, M. I. F., M. U. Rosli, Muhammad Ikman Ishak, M. S. Zakaria, Mohd Riduan Jamalludin, C. Y. Khor, WM Faizal WA Rahim, M. A. M. Nawi, and Suhaimi Shahrin. "Simulation based optimization of injection molding parameter for meso-scale product of dental component fabrication using response surface methodology (RSM)." In *AIP Conference Proceedings*, vol. 2030, no. 1, p. 020078. AIP Publishing LLC, 2018. https://doi.org/10.1063/1.5066719